AIAA-2003-0211

Enhanced Airfoil Design Incorporating Boundary Layer Mixing Devices

Michael Kerho and Brian Kramer
Rolling Hills Research Corporation
Torrance, CA

**41st AIAA Aerospace Sciences
Meeting & Exhibit
6-9 January 2003 / Reno, NV**

American Institute of Aeronautics and Astronautics

Enhanced Airfoil Design Incorporating Boundary Layer Mixing Devices

Michael F. Kerho[†] and Brian R. Kramer[*]
Rolling Hills Research Corporation
3425 Lomita Blvd.
Torrance CA 90505

Abstract

The purpose of this study is to design an extended run, robust natural laminar flow (NLF) airfoil section using boundary-layer mixing devices (BLMDs). Both analytical and experimental investigations were conducted. The enhanced mixing effect of the BLMDs was incorporated in an existing airfoil design code. The zonal interactive viscous/inviscid program XFOIL was modified to include the effect of vortex generators. After initial calibration and verification of the baseline design codes accuracy, the boundary-layer treatment in the code was modified to include the enhanced mixing effect of the vortex generators. Airfoil designs were generated based on the modified code. These designs included airfoil sections having upper surface laminar run extents of 75% to 85% chord. These sections were then wind tunnel tested at Reynolds numbers from 500,000 to 2.0×10^6. Results from this investigation have produced a viable airfoil design tool for sub-critical airfoil sections that can include the effect of vortex generators. The airfoil sections designed provide a realizable performance enhancement over traditionally designed NLF sections.

Nomenclature

c	Model chord length
C_D	Dissipation Coefficient
C_f	Skin Friction Coefficient
C_τ	Shear Stress Coefficient
δ	Boundary Layer Thickness
δ^*	Displacement Thickness
H	Shape Factor $= \delta^*/\theta$
θ	Momentum Thickness
u_e	Boundary-Layer Edge Velocity
U_{vg}	Velocity in the undisturbed boundary-layer at the VG height
k_{vg}	BLMD device height
Re	Reynolds Number
Re_{kvg}	VG Reynolds Number
$Re_{k,cr}$	Critical roughness Reynolds number to promote transition

---

[†] Chief Aerodynamicist, Senior Member AIAA
[*] President, Senior Member AIAA

Introduction

The advantages of NLF airfoils can be enhanced by including in the original design a miniature Boundary Layer Mixing Device (BLMD) that allows airfoil sections to be designed with a much more aggressive pressure recovery profile. The advantage of such a design is an increase in the percentage of laminar flow, and hence reduced drag at an increased design lift coefficient. The increase in lift to drag ratio (L/D) will increase the performance of high altitude vehicles and can help to reduce the vehicle size, and hence the cost, required to carry a fixed weight payload.

Aircraft flying at extremely high altitudes face a number of challenges, many caused by the low atmospheric density. At altitudes from 60,000 to 100,000 feet, and above, the dynamic pressure at high subsonic speeds is not adequate to support a conventional aircraft and requires a very efficient wing design. In the case of a high altitude sensor platform, the wing is sized to begin its cruise at the minimum acceptable altitude (at the airfoil's design lift coefficient, C_L), and then it is allowed to cruise climb as fuel weight is burned off. A particular airfoil is designed to operate in a range of design C_L's, so the highest part of this range is used for the initial cruise

American Institute of Aeronautics and Astronautics

and a value near the lowest part will be needed at the end of the cruise. In general, if a higher initial altitude or payload is required, a larger wing is needed. Particularly with the requirement for a sizable payload, increasing the size of a conventional wing to support the aircraft will lead to greater structural weight, which in turn will drive the wing even larger. This spiral of diminishing returns quickly leads the aircraft designer to realize that some significant increase in performance must come from greatly decreased structural weight through the use of composites, increased propulsion system efficiency, or increased aerodynamic efficiency.

While high altitude flight brings many increased challenges, it also brings a unique opportunity. As altitude increases, the Reynolds number decreases substantially. The opportunity that this presents is a chance to take advantage of the dramatic drag decrease offered by laminar flow airfoil sections. The advantages of laminar flow have been known and studied for many years. However, the single greatest reason that laminar flow technology has not been widely applied is that NLF is very difficult to maintain at the high Reynolds numbers present at typical flight conditions. At higher Reynolds numbers, the boundary layer is much more susceptible to transition due to contamination from dirt, bugs and precipitation. In addition, manufacturing tolerances and surface quality issues have made these types of designs cost prohibitive. The lower Reynolds numbers present at high altitudes make natural laminar flow airfoil designs much more appealing. The longer the chordwise extent of laminar flow on an airfoil, the greater the benefit will be. The difficulty with an airfoil design which has an extended laminar run is in providing a rapid pressure recovery without inducing boundary layer separation. Generally, the extent of laminar flow on either the upper or lower surface is governed by the chord length required to properly recover the pressure at the trailing-edge. Most NLF airfoils have a small separated region downstream of the laminar run at the onset of the pressure recovery region. The small separated region is termed a laminar separation bubble. The larger the magnitude of the pressure recovery, the larger the size of the separation bubble. The limit being separation without reattachment by the trailing-edge. While the presence of a laminar separation bubble has only minor effects on the sectional lift, it can produce significant increases in profile drag, undermining the beneficial effects of the laminar flow. Generally, a balance between the extent of the laminar run and the size of the separation bubble is found that exploits the laminar benefits while minimizing the effects of the separation bubble. It may be possible, however, to design an airfoil with an extremely long laminar run, followed by an accelerated pressure recovery with no separation

bubble. The accelerated pressure recovery will remain attached and fully recover by the trailing-edge with the aid of enhanced mixing in the form of sub-boundary-layer sized mixing devices. Such an aggressive pressure profile will not only decrease the section drag, but the additional length of negative pressure on the airfoil's upper surface will increase the section's lift.

Boundary-layer mixing devices in the form of vortex generators are currently used throughout the aircraft industry. They are generally used to prevent or lessen the severity of boundary-layer separation. Vortex generators are termed a passive flow control device since they are fixed in both location and size and do not require additional power to operate. Historically, however, vortex generators are not included in the initial design process and are only used after undesirable flow characteristics have been observed. This study attempts to change the "band-aid" nature of vortex generator installation by including them in the initial design process and taking advantage of their beneficial effects early in the design process. A schematic showing streamlines for a typical NLF airfoil design and an enhanced NLF design, with and without flow control, is shown in Figure 1. The pressure distribution and drag polar for a typical NLF airfoil and an enhanced NLF design are shown in Figure 2. From Figure 2, the extended rooftop and much steeper pressure recovery of the enhanced section is clearly evident. For the design shown, the enhanced section results in a significant drag reduction across the width of the bucket. The effect of increased laminar run can be estimated using simple laminar and turbulent boundary-layer skin friction approximations with appropriate weighting factors. Figure 3 shows the reduction in drag corresponding to various amounts of laminar flow. The baseline NLF airfoil assumes a 50% laminar run on the lower surface. Zero form drag is assumed. From Figure 3, as the extent of upper surface laminar run is increased, the percent reduction in C_{d0} also increases. Increasing the laminar run from 60% to 70% on the upper surface, for example, would yield a 4.4% reduction in C_{d0}, which could be doubled if the lower surface laminar run were also extended by 10%. It should be noted that the reduction in C_{d0} shown in Figure 3 is based on skin friction only. If the vortex generators can be used to extend the laminar run and also eliminate the separation bubble, a further decrease in C_{d0} will result from a reduction in form drag due to the elimination of the bubble. As with any airfoil design, the process involves finding the correct balance between several competing factors, the amount of laminar run, separation bubble size and location, skin friction, form drag, and section thickness for example.

2

In order to fully exploit the benefits of vortex generators in the design process, the effect of the enhanced mixing needs to be incorporated in a design approach. For this project, the enhanced mixing effect of the BLMDs was incorporated in an existing airfoil design code. The zonal interactive viscous/inviscid program XFOIL was chosen as the airfoil design code to be modified. The XFOIL code uses a linear-vorticity stream function panel method coupled with an integral boundary-layer formulation. The code incorporates a Karman-Tsien compressibility correction, which gives accurate flow predictions up to sonic conditions but will not predict shock waves. XFOIL has proven accurate in the low to moderate Reynolds number regime and can predict transitional separation bubbles and mild trailing-edge separation. The code contains a laminar/turbulent transition criterion using spatial amplification theory with an e^N prediction method, allowing the design of NLF sections.

Enhanced Mixing Effect on The Boundary-Layer

Boundary-layer mixing devices in the form of vortex generators were first used by H.D. Taylor at United Aircraft in 1948 to prevent boundary-layer separation in a wind tunnel diffuser.[1] The first systematic study of vortex generators and their effect on the boundary-layer was performed by Schubauer and Spangenberg in 1959.[2] Vortex generators have since been used extensively both internally and externally on aerodynamic surfaces to prevent or lessen the effects of boundary-layer separation in adverse pressure gradients. The action of a vortex generator is to generate a streamwise vortex that mixes energetic outer layer fluid with the less energetic near wall fluid. If properly situated in the boundary-layer, the helical motion of the vortex forces higher energy fluid of the free-stream or core flow into the slower moving fluid of the boundary-layer. The re-energized boundary-layer flow is now more able to negotiate much steeper and higher pressure rises and is thus more resistant to flow separation.[3]

The primary boundary-layer variables of interest are the displacement thickness, momentum thickness, shape factor, and skin friction. The displacement thickness, momentum thickness, and shape factor are integral parameters based upon the shape of the velocity profile. The displacement thickness, δ^*, is a measure of the amount the outer, inviscid dominated flowfield is displaced by the presence of the viscous boundary-layer. The momentum thickness, θ, is a measure of the amount of momentum lost by the flow due to the presence of the viscous boundary-layer. The shape factor, H, is a ratio of the displacement to momentum thickness. These three integral parameters allow

examination of the state of the boundary-layer and the effect of mixing on the mean flow without becoming involved with the detailed flow processes.[2] The final parameter of interest is the skin friction, C_f. The effect of increased mixing in a boundary-layer can be observed in the transition from laminar to turbulent flow. In a laminar boundary-layer, momentum transfer and mixing is accomplished through molecular diffusion. In a turbulent boundary-layer, however, mixing and momentum transfer within the boundary-layer are accomplished at a much greater rate through a bulk momentum transfer. As fluid flows over a wall bounded surface, the retardation of the flow by viscous forces causes both the momentum and displacement thickness to grow. In a laminar boundary-layer, $\theta \approx 0.30\delta^*$, increasing to $\theta \approx 0.80\delta^*$ after transition. The enhanced mixing in the turbulent boundary-layer brings higher speed fluid closer to the wall increasing the momentum thickness and skin friction. During the transition process, the introduction of turbulence occurs over such a short streamwise distance that θ remains virtually unchanged. The enhanced mixing, however, is immediately visible in a reduced δ^*. This change in the relationship between the displacement and momentum thickness is best observed in the well-known change in the shape factor H. The reduction in displacement thickness results from the momentum loss being more evenly dispersed throughout the boundary-layer due to the enhanced mixing.[2] These changes are illustrated by looking at the change in δ^*, θ, H and C_f for a naturally transitioning boundary-layer on simple airfoil section. The boundary-layer parameters computed by XFOIL for a NACA 0005 at Re=3.0×10^6 and an angle-of-attack of 1.0° are shown in Figure 4. From Figure 4, the dramatic drop in displacement thickness and resulting change in the shape factor due to the increased mixing in the turbulent boundary-layer are clearly evident. Also, the abrupt increase in skin friction as a result of higher velocity fluid being brought closer to the wall is depicted.

These same effects are seen to occur with the enhanced mixing provided by vortex generators. The increased fluid entrainment and mixing provided by the generators will generally result in a decrease in the displacement thickness with an accompanying increase in the momentum thickness. The shape factor will therefore also be reduced. In addition to the changes in the integral parameters, an increase in the skin friction is also observed.[4] The increase in momentum thickness is not only due to the increased mixing, but also from a price paid to generate the vortex itself. These effects are illustrated in Figure 5. The enhanced mixing re-energizes the retarded near wall flow allowing steeper adverse gradients to be negotiated. After modification

3

of the XFOIL code to include the effect of the mixing devices, the integral boundary-layer parameters will help provide confirmation that the code modifications produce the desired physical effects on the flowfield. Although XFOIL is a 2D design code and the vortex generators yield a locally 3D flowfield, if properly spaced along the airfoil span, their global effect can be 2D. This assumption was verified experimentally and will be shown later.

XFOIL Boundary-Layer Formulation

The boundary-layer formulation used in XFOIL is a compressible lag dissipation integral method. The information presented here on its development is taken from Drela and Giles[5]. The viscous and inviscid layers are coupled through the displacement thickness. The entire non-linear viscous and inviscid equation set is solved simultaneously as a fully-coupled system by a global Newton-Raphson method. The integral formulation uses a two-equation dissipation type closure for both the laminar and turbulent portions of the boundary-layer. A lag equation is added to the turbulent formulation to account for lags in the response of the turbulent stresses to changing flow conditions. The two-equation method is used over simpler one equation models (Thwaites') due to its ability to predict thin separated regions such as separation bubbles. For laminar closure, Falkner-Skan profiles are assumed. For turbulent closure, the skin friction and velocity profiles of Swafford[6] are used. The dissipation coefficient and shear stress are derived from the locus of equilibrium turbulent boundary-layers postulated by Clauser[7]. The primary boundary-layer variables used in XFOIL are u_e, θ, δ^*, and $C_\tau^{1/2}$.

XFOIL Boundary-Layer Modifications

In order to include the enhanced mixing effect of vortex generators in the XFOIL design and analysis code, the boundary-layer formulation in XFOIL was modified. Specifically, turbulence production in the turbulent boundary-layer formulation was enhanced by modifying the stress transport formulation. The rate equation is modified (increased) at the location of the vortex generators and decreases exponentially downstream of this location. Increasing the rate equation at the vortex generator location produces a decrease in the local displacement thickness and increase in both the momentum thickness and skin friction. The method involves modifying the dissipation coefficient C_D through the shear stress coefficient C_τ. The XFOIL code was modified to include an amplification of the rate equation at the location of the vortex generators. The amplification factor provides a step function increase at the location

of the generators and decays exponentially downstream. The decay in amplification was chosen to mimic the downstream decay in shed vorticity generated by a mixing device. The model has been calibrated for use with a single row of co-rotating vortex generators with a height to length ratio of 4, local VG angle-of-attack of 20°, and a spanwise spacing of 8 VG heights. These conditions were experimentally verified to produce a 2-D effect on the overall flowfield.

The XFOIL program was modified so that the user can add the vortex generator effect in the analysis portion of the code. Vortex generators can be added at any chordwise location on either the upper or lower surface, or on both surfaces. Since only the turbulent boundary-layer formulation was modified, the enhanced mixing effect is only modeled in a turbulent boundary-layer. As a result, vortex generators placed in a laminar boundary-layer that do not transition the flow are not modeled. This is a reasonable assumption since in order to obtain the most benefit from a mixing device, its mixing effect should be complimented by the natural mixing produced by a turbulent boundary-layer. One key function of the enhanced mixing model is the ability to predict vortex generator induced transition as a function of local flow conditions.

Since the boundary-layer thickness, separation bubble location and extent are a function of Reynolds number and angle-of-attack, the height of the VGs with respect to the boundary-layer varies with these parameters, as does their ability to not only promote vortex induced mixing, but also to promote transition/turbulent boundary-layer induced mixing. In order for a VG model to be physically consistent, it must account for changes in the local flow conditions. An easy fix to this problem would be to just employ overly large VGs to ensure transition and increased mixing for all cases of interest. This would be counter productive, however, to the design of a low drag section. As a result, a transition prediction model was been added to the modified code.

The unmodified version of XFOIL employs a spatial-amplification theory based on the Orr-Sommerfeld equation for transition prediction. The transition model is basically an e^N prediction method. The e^N method assumes that transition occurs when the most unstable Tollmein-Schlichting wave in the boundary-layer has grown by a given factor, e^N, where N is usually taken to be 9. The amplification factors can be calculated knowing the local laminar boundary-layer parameters. The laminar boundary-layer in XFOIL is calculated using the Falkner-Skan profile family. This is a family of self-similar profiles which take both favorable and adverse pressure gradients into account. Using the

4

Falkner-Skan profile family, the Orr-Sommerfeld equation has been solved for the spatial amplification rates of a range of boundary-layer conditions (shape factors, pressure gradients, etc….). From these solutions an empirical transition formula has been generated as a function of local boundary-layer conditions. The code basically predicts transition by comparing the current boundary-layer conditions to the empirical model. While this method works very well for natural, Tollmein-Schlichting based transition, it does not allow for roughness or VG based bypass transition modes. The basic XFOIL code does allow transition forcing to be specified at a given chordwise location, but the forcing is merely a switch and assumes the flow will transition by some artificial means for all conditions. For the current VG model to accurately predict the VGs effect on the boundary-layer, a transition prediction model is required that will determine if the VGs will promote a bypass type transition at the VG location based on the current boundary-layer parameters as the relative height of the VG in the boundary-layer changes with changing conditions.

VGs are basically a specialized form of distributed, or isolated roughness. A transition prediction model has been incorporated into the XFOIL code which determines the VG roughness based Reynolds number, Re_{kvg} to determine if the current height of the VG in the boundary-layer is sufficient for the VG to promote a bypass transition. For this definition $Re_{kvg}=U_{vg}\rho k_{vg}/\mu$, where U_{vg} is the velocity in the undisturbed boundary-layer at the height of the VG, k_{vg}. The value of Re_{kvg} for the roughness location is then compared to the critical Reynolds number value to determine if transition will occur. Since the chordwise location and height of the VG are known, all that is needed is U_{vg}, the velocity in the undisturbed boundary-layer at the height of the VG. At the VG location, individual velocity profiles are generated based upon the integral parameters. From these profiles, U_{vg} is determined allowing the calculation of Re_{kvg}. The VG roughness Reynolds number is then compared to the critical Reynolds number to determine if the VG height is sufficient to promote transition. If so, transition is fixed in the code at the VG location and the VGs mixing effect is included in the boundary-layer model. If the VG height is insufficient to promote transition, no modification to the boundary-layer model is made. This system allows various conditions and Reynolds numbers to be run for a fixed VG height and location, as is experienced in real life.

The code logic of the transition prediction methodology works by first obtaining a converged solution for the clean airfoil case. This clean solution is saved to memory and the boundary-layer at the VG location is calculated and tested to determine if the VG height is sufficient to promote a bypass transition. If the VG height is sufficient to produce an $Re_{k,cr}$ of 600, transition is said to occur and the solution is recalculated with forced transition and enhanced mixing at the VG location. After the VG solution has been converged on, the previous clean solution is loaded back into memory for next condition. In addition to the VG model, the modified code can be used to accurately predict boundary-layer trip effects across a range of Reynolds number and angles-of-attack.

Modified XFOIL Test Cases

As a test of the modified code, a NACA 0001 section was run at $Re=1\times10^6$, $\alpha=0°$. The NACA 0001 section is basically a flat plate with zero pressure gradient allowing a simple boundary-layer to be generated. The NACA 0001 section was run with and without vortex generators placed at 50% chord. Transition was fixed at the leading-edge. Boundary-layer parameters were analyzed to determine if the modified boundary-layer exhibited the desired effects downstream of the generator location. These results are shown in Figure 6. From Figure 6, the increased fluid entrainment and mixing provided by the vortex generators is shown to produce a reduction in the shape factor and increase in the skin friction. From Figure 6, the modifications to the XFOIL turbulent boundary-layer formulation appear to be producing the desired mixing effects.

Traditionally VGs have been used to prevent or delay separation for increased C_{lmax}. They are usually placed around 20-30% chord with a height roughly equivalent to the local boundary-layer thickness. Experimental results for a GA(w)-2 section were available with and without co-rotating VGs placed at the 30% chord location. The VGs were sized to be on the order of the local boundary-layer thickness at $Re=2.2\times10^6$. The modified XFOIL code was used to predict the effects of placing VGs at the 30% chord location on a GA(W)-2 section. From Figure 7, the modified XFOIL results predict the increase in C_{lmax} due to the presence of the vortex generators relatively well. The modified code, however, does under predict the device drag due to the generators. At the higher C_l's, prior to separation, the modified code also predicts lower drag than the baseline clean case. Although there is an increase in skin friction due to the presence of the VGs, their reduction of the displacement thickness results in a reduction in form drag which is greater than the local increase in skin friction. Overall, from Figure 7, the modified code appears to be predicting the overall effect of the VGs fairly well.

5

Extended Run Laminar Designs

Several extended run laminar airfoil sections have been designed and tested using the modified XFOIL code. As with any airfoil design, the process involves finding the correct balance between several competing factors such as minimum drag, required C_{lmax}, and allowable pitching moment. The design process required carefully weighing tradeoffs between the amount of laminar run, separation bubble size and location, skin friction, form drag, and section thickness just to name a few. The purpose of the current study was verify that extended laminar run sections could be designed that produced realizable gains over existing NLF sections. Could sections be designed that offered increased laminar flow extents with reduced separation bubble sizes that offered increased performance? The design process was a study in the tradeoffs between reduced skin friction and increased form drag. Without the enhanced mixing of vortex generators, increasing the laminar run and severity of the adverse recovery gradient simply increases the size of the separation bubble and resulting form drag. The key was to extend the laminar run and use the vortex generators to eliminate the separation bubble and produce a thin, healthy turbulent boundary-layer with an acceptable level of profile drag. Even with the enhanced mixing of vortex generators, it is relatively easy to design a section with extended laminar flow that eliminates the separation bubble, remains attached to the trailing-edge but has poor performance due to a thick boundary-layer and overly large profile drag.

Although several sections were designed and tested, only one section will be described in detail here. In order to provide a baseline for comparison, the section was based on the NASA NLF(1)-1015 section designed by Maughmer and Somers[8]. The NLF(1)-1015 section was designed as a high-altitude, long endurance airfoil. The airfoil is unflapped and has a thickness of 15% chord. The design Reynolds number range was $0.7x10^6$ to $2x10^6$. The section was designed to have low drag for lift coefficients ranging from 0.4, which corresponds to a high-speed dash, to 1.5, the maximum endurance condition. This section has both upper and lower surface separation bubbles across the design range of C_ls. Both the upper and lower surface have extensive laminar runs across a wide range of the drag bucket from C_l=0.4-1.4 with transition occurring at approximately 70% chord on both surfaces with separation bubbles present from $x/c \approx 0.625$ to $x/c \approx 0.75$ on the upper surface and $x/c \approx 0.60$ to $x/c \approx 0.70$ on the lower surface.

The new section, EID75SR was designed to maintain the NLF(1)-1015 lower surface and only modify the upper surface downstream of 40% chord. The EID75SR section was designed to modestly increase the upper surface laminar run to x/c=0.75 and attempt to recover with no separation bubble. The design conditions for the section were C_l=1.0 and Re=$0.7x10^6$. For this section relatively mild vortex generators were placed at x/c=0.75 to enable a separation free recovery. The vortex generators were prescribed as co-rotating with a rectangular planform and k_{vg}/c=0.0025 (nominally 0.5δ) with a length to height ratio of 4 and a spanwise spacing of 8. The airfoil sections are shown in Figure 8 with pressure distributions at the design conditions, C_l=1.0 and Re=$0.7x10^6$. From Figure 8, the aggressiveness of the adverse pressure recovery becomes increasingly severe as transition is pushed aft. Predicted lift and drag polars for the baseline NLF and new EID75SR sections are shown in Figure 9. From Figure 9, other than a slightly lower C_{lmax}, the EID75SR and NLF(1)-1015 sections differ little in their lift characteristics. At higher angles-of-attack, due to the far aft location of the vortex generators, after transition has moved forward of the VG location and the turbulent boundary-layer thickness has increased, the effectiveness of the VGs decreases, resulting in a slightly lower C_{lmax}. The extended laminar run does produce a noticeable drag reduction across the polar. At Re=$7x10^6$, the modified XFOIL program predicts an 8% drag reduction at C_l=1.0 for the EID75SR section as compared to the baseline NLF(1)-1015 section. Overall, the EID75SR section appears to provide benefits over the baseline section.

Experimental Results

The baseline model NLF(1)-1015 and EID75SR sections were tested in the University of Illinois low-speed wind tunnel at Reynolds numbers from $0.5x10^6$ to $2.0x10^6$. Force and moment, surface pressure, and fluorescent oil flow visualization data were obtained for each section. Lift and pitching moment coefficients were calculated by integrating the model surface pressures and drag coefficients were obtained through the use of a 40 port traversing wake rake placed 1 chord length downstream of the model.

Prior to testing the EID75SR section with vortex generators, the clean model was thoroughly tested. Since the VG model currently incorporated in the code is designed to enhance the mixing of the original or clean boundary-layer, if the original boundary-layer is not accurately predicted, the VG model will only enhance the mixing of an already inaccurate solution. Lift and drag polars and surface pressures for the clean EID75SR section at Re=$0.7x10^6$ are shown in Figure 10

American Institute of Aeronautics and Astronautics

and Figure 11. From Figure 10 and Figure 11, XFOIL appears to predict the characteristics of the clean EID75SR section well. The XFOIL predicted bubble location and extent compare well with the measured pressures. Fluorescent oil flow visualization results for the clean section at $\alpha=0°$, Re=0.7x106 shown in Figure 12 show that the separation bubble was 2-D and well behaved.

Results for the 0.5δ co-rotating VGs at Re=0.7x10^6 are shown in Figure 13 and Figure 14. From Figure 13, the experimental and predicted lift curve results for the EID75SR section with VGs compare well with a slight under prediction of C_{lmax}. The experimental C_{lmax} for the EID75SR and NLF(1)-1015 sections compared well. The drag results are shown in Figure 14. From Figure 14, the EID75SR section produced a drag reduction of 7.5 counts at the design C_l =1.0, as compared to the NLF(1)-1015 experimental data. The original predicted drag reduction for the EID75SR section was 7 counts. The lower bounds of the drag bucket were over predicted by XFOIL for both the EID75SR and NLF(1)-1015 sections. Transition appears to have been moving forward prematurely on the lower surface for both sections. Since the lower surface for both models was cast from the same mold, the premature transition could be a result of a model quality issue. Overall, however, the modified code predicted the VG behavior quite well and yielded a net drag reduction at the design C_l of approximately 7.5 counts. A plot of the surface pressures at C_l=1.0 for the NLF(1)-1015 section and the EID75SR section with and without VGs is shown in Figure 15. From Figure 15, the NLF(1)-1015 section is observed to have a large separation bubble extending from x/c≈0.60 to x/c≈0.70. The clean EID75SR had a large separation bubble extending from x/c≈0.74 to x/c≈0.86. The EID75SR section with VGs, however, appears to have been fully attached with no separation. Flow visualization results for the EID75SR section with the co-rotating 0.5δ VGs at x/c=0.75 for $\alpha=0°$ are shown in Figure 16. From Figure 16, the individual vortices created by the VGs are clearly visible. The flow was completely attached with no separation bubble at $\alpha=0°$ and is 2-D in nature. As discussed in the Introduction and Boundary Layer Modifications sections, although the local flowfield of the individual vortex generators is 3-D, through proper spacing the global effect can be 2-D in nature. The results for the EID75SR section are very promising. The results show that the effect of the VGs can be predicted and taken advantage of for an increased laminar run section.

Experience with the modified code indicates that the extended laminar run designs seem to perform better at lower Reynolds numbers where the associated laminar separation bubbles are larger with more severe drag consequences. One drawback to the use of vortex generators for boundary-layer mixing is the fact that they are a passive flow control device. Their size and location on the airfoil is fixed. As a result, they function better for a point design at a given Reynolds number. For off design conditions, higher or lower Reynolds numbers, the height of the vortex generator changes in the boundary-layer. If the vortex generator becomes too large, it's device drag will also become large and possibly out weight its benefits. If the vortex generators are too small, they will loose effectiveness. Results from this study show that a vortex generator sized to be approximately half the height of the local boundary-layer will produce a good combination of enhanced mixing with low device drag.

Conclusions and Recommendations

The purpose of this study was to design an extended run (NLF) airfoil section using boundary-layer mixing. The advantages of NLF airfoils can be enhanced by including in the original design a miniature Boundary Layer Mixing Device (BLMD), in this case vortex generators, that allow airfoil sections to be designed with a much more aggressive pressure recovery profile. The advantage of such a design is an increase in the percentage of laminar flow. The key to the current study was to determine if the benefits of vortex generators could be exploited from the onset of a design process and be incorporated in the design from the beginning. In order to accomplish this task, an airfoil design program was modified to include the enhanced mixing effect of vortex generators in its design and analysis routine.

The zonal interactive viscous/inviscid program XFOIL was modified to include the effect of vortex generators. The code was modified by enhancing the turbulence production in the turbulent boundary-layer formulation. Turbulence production was enhanced by modifying the stress transport formulation. The rate equation was modified (increased) at the location of the vortex generators and decreases exponentially downstream of this location. Increasing the rate equation at the vortex generator location produced a decrease in the local displacement thickness and an increase in both the momentum thickness and skin friction, mimicking the effect of a vortex generator.

Several airfoil sections were designed and tested with the modified XFOIL code. From these designs it was shown that an airfoil section could be designed with an extended laminar run on the upper and lower surface using vortex generators in the design process to produce

American Institute of Aeronautics and Astronautics

a section with no laminar bubble or trailing-edge separation. If designed correctly, the sections showed that they could produce a realizable performance increase over a traditionally designed NLF section. The EID75SR section is an example of this, yielding a net drag reduction of 8%.

The use of active synthetic jets instead for vortex generators could significantly enhance the performance and capabilities of the extended run NLF sections. By incorporating active synthetic jets, the enhanced mixing can be tailored to individual conditions throughout the flight envelope yielding maximized performance at several operating conditions. Since the zero net mass flux jets are buried within the wing surface, the section also has low radar cross section capabilities. Finally, the amount of enhanced mixing can be controlled real time. The amount of mixing will change the aft flow and separation characteristics of the airfoil, creating a different virtual shape for each setting. Also, by varying the amount of mixing along the span of the wing, variations in the lift distribution can be created to generate hinge-less, pilot reactive roll control.

Acknowledgements

References

[1] Taylor, H. D., "Design Criteria For And Applications Of The Vortex Generator Mixing Principle," Report M-15038-1, United Aircraft Corporation Research Department, Feb. 1948.

[2] Schubauer, G. B., and Spangenberg, W. G., "Forced Mixing in Boundary Layers", Journal of Fluid Mechanics , Vol 8, Part 1, May 1960, pp. 10-32.

[3] Wednt, B. J., and Reichert, B. A., "The Modeling of Symmetric Airfoil Vortex Generators," AIAA-96-0807, or NASA CR 198501, June 1996.

[4] Inger, G. R., and Siebersma, T., "Computational Simulation of Vortex Generator Effects on Transonic Shock/Boundary-Layer Interaction," Journal of Aircraft, Vol. 26, No. 8, August 1989, pp. 697-698.

[5] Drela M., and Giles, M. B., "Viscous-Inviscid Analysis of Transonic and Low Reynolds Number Airfoils," AIAA Journal, Vol. 25, No. 10, October 1987, pp. 1347-1355.

[6] Swafford, T. W., "Analytical Approximation of Two-Dimensional Separated Turbulent Boundary-Layer Velocity Profiles," AIAA Journal, Vol. 21, June 1983, pp. 923-926.

[7] Cluaser, F. H., "Turbulent Boundary Layers in Adverse Pressure Gradients," Journal of the Aeronautical Sciences, February, 1954, pp. 91-108.

[8] Maughmer, M. D., and Somers, D. M., "Design and Experimental Results for a High-Altitude, Long-Endurance Airfoil," Journal of Aircraft, Vol. 26, No. 2, Feb. 1989, pp.148-153.

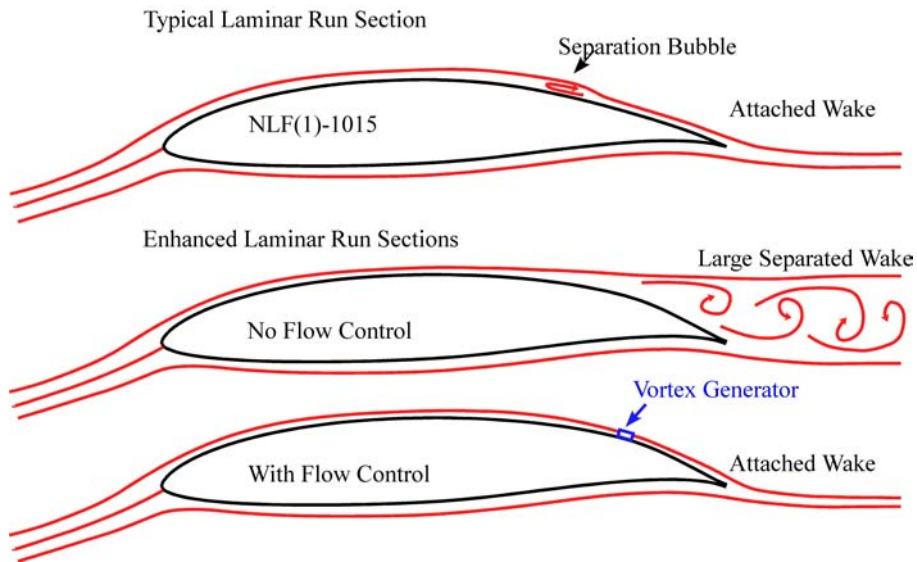American Institute of Aeronautics and Astronautics

Figure 1: Schematic showing the flowfield streamlines of a typical natural laminar flow section and an enhanced laminar flow section with and without flow control.
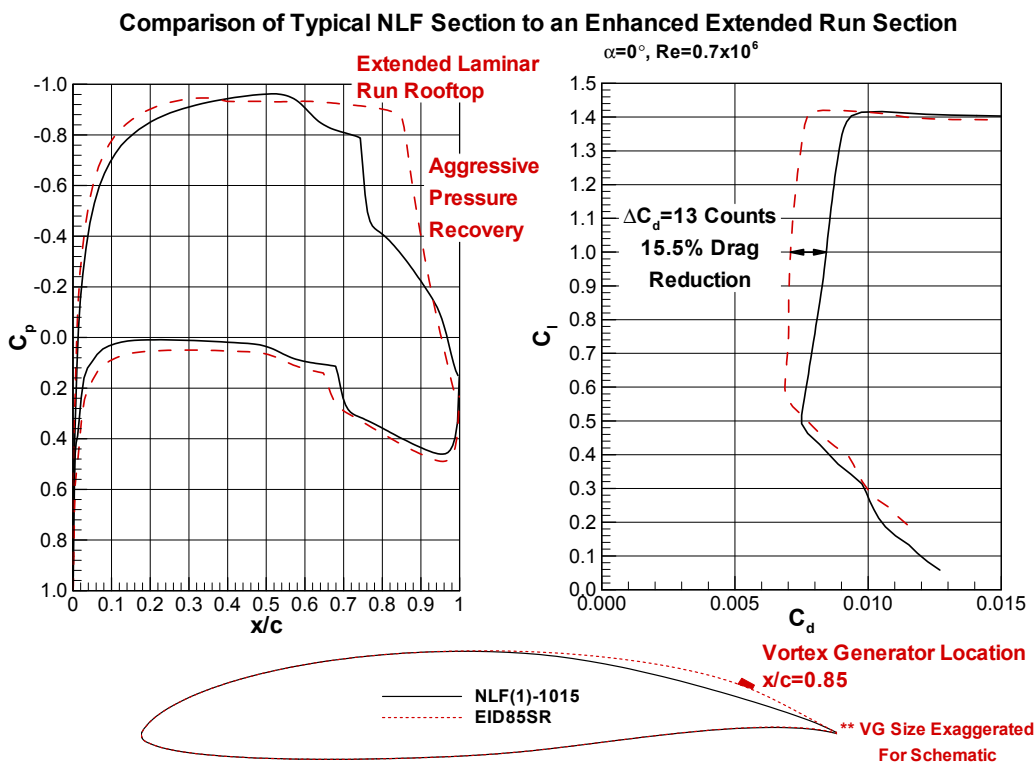

Figure 2: Comparison of the pressure distribution and drag polar for a typical NLF and an enhanced NLF design showing the aggressive pressure recovery and reduced drag across the width of the bucket.
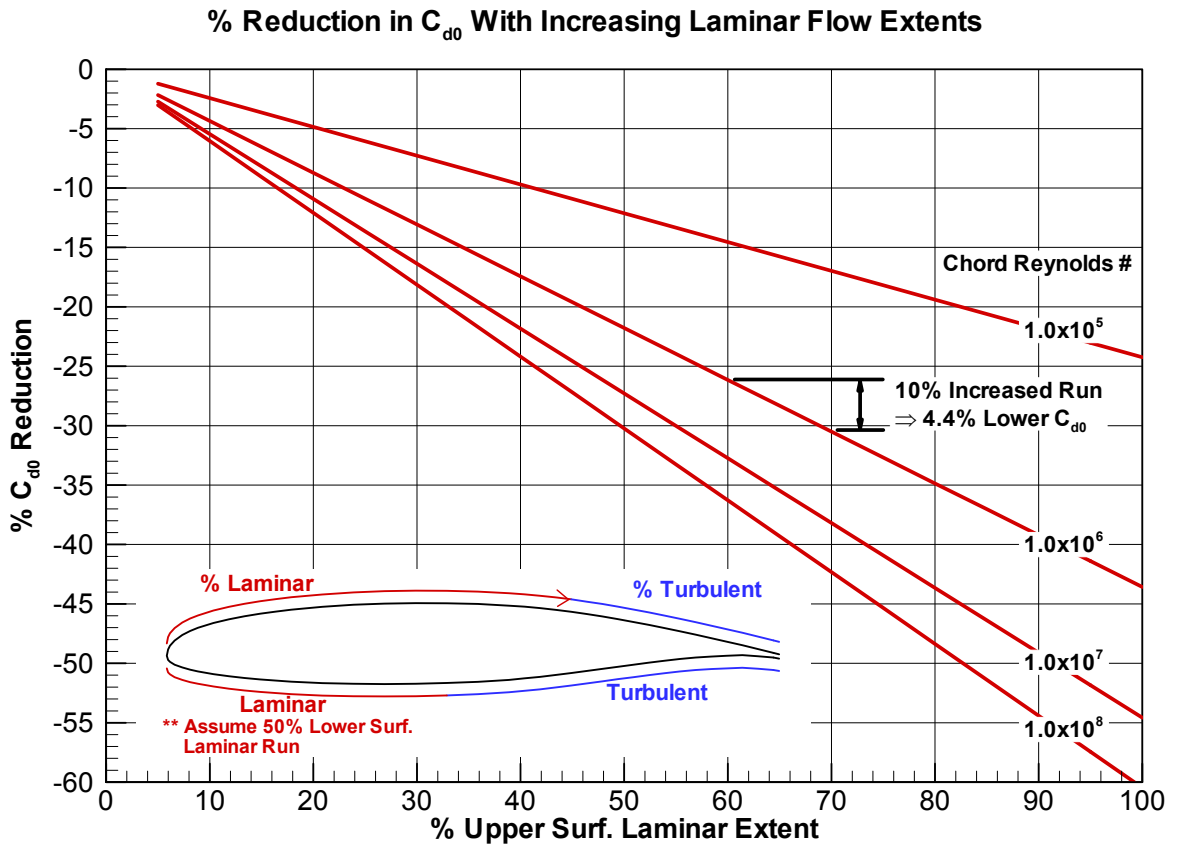
9

American Institute of Aeronautics and Astronautics

Figure 3: Percentage reduction in C_{d0} with increasing laminar flow extents assuming zero form drag. Baseline case assumes 50% laminar run on the lower surface.
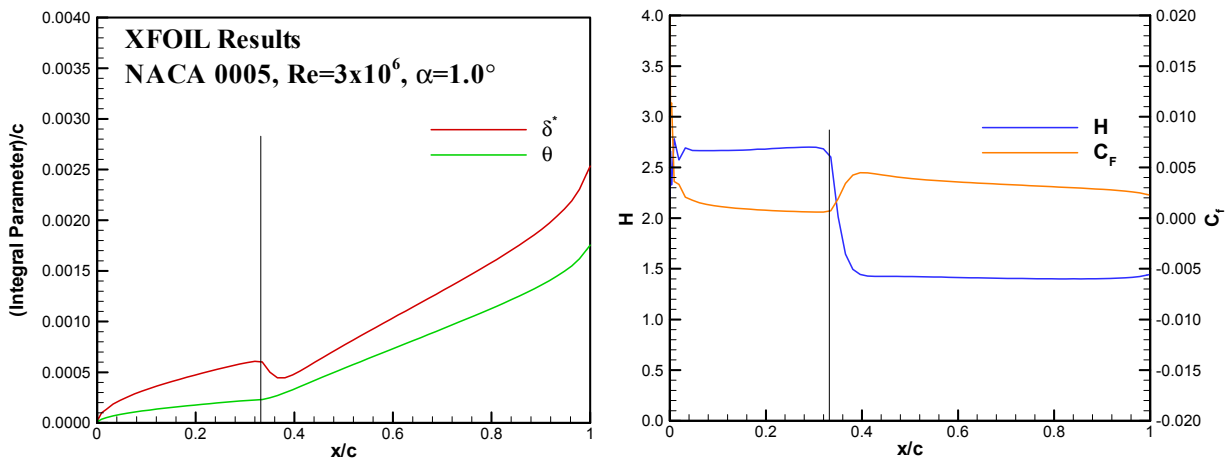
Figure 4: Change in boundary-layer parameters due to transition for a NACA 0005, Re=3x10^6, α=1.0°.

American Institute of Aeronautics and Astronautics
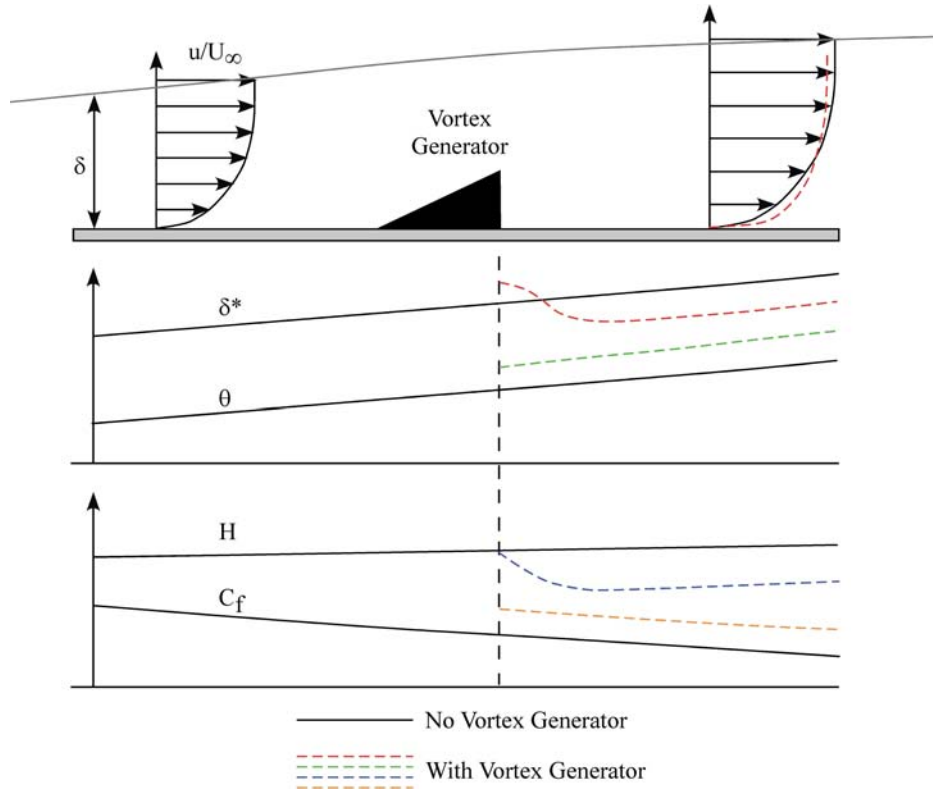
Figure 5: Schematic of the observed changes in boundary-layer parameters due to the enhanced mixing produced by a vortex generator.
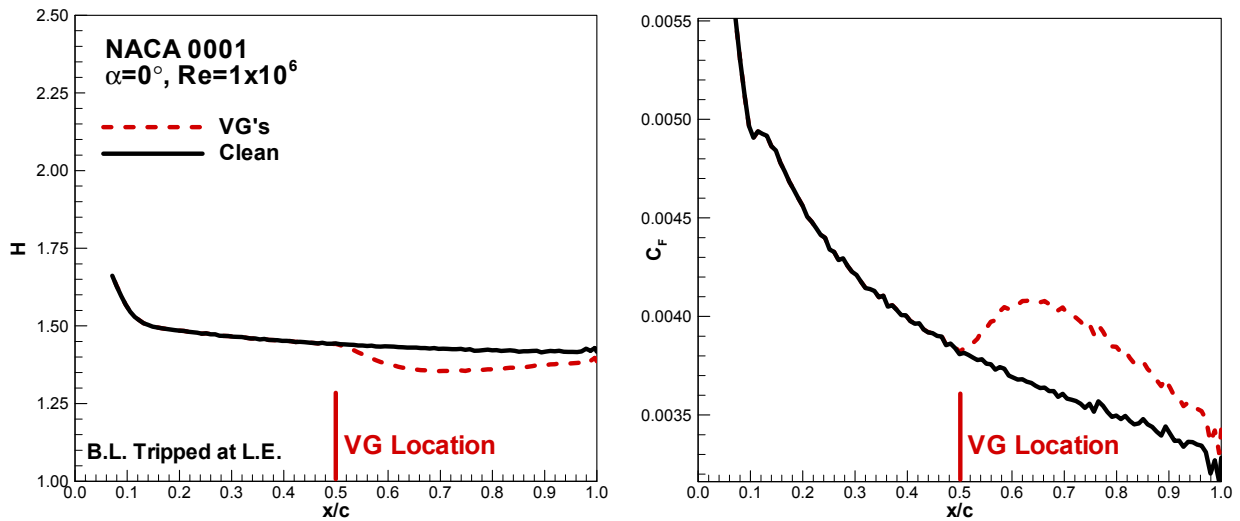
Figure 6: Modified XFOIL predictions of the effect of vortex generators on the shape factor and skin friction for a turbulent boundary-layer.
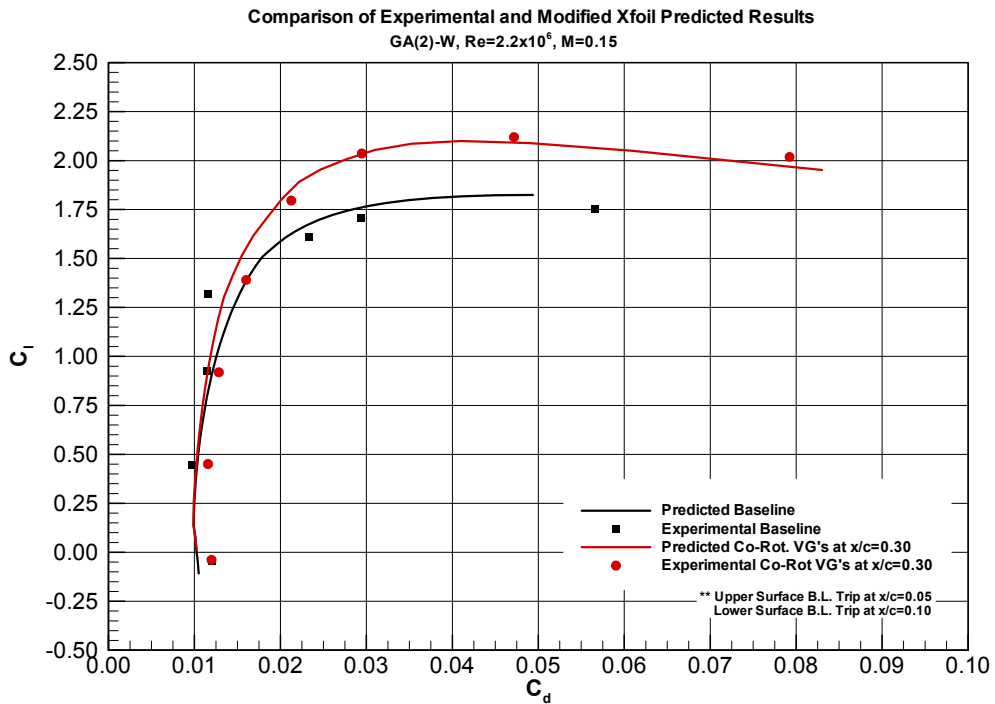
Figure 7: Comparison and experimental and modified XFOIL predicted results for a GA(W)-2 section with and without co-rotating vortex generators placed at 30% chord.
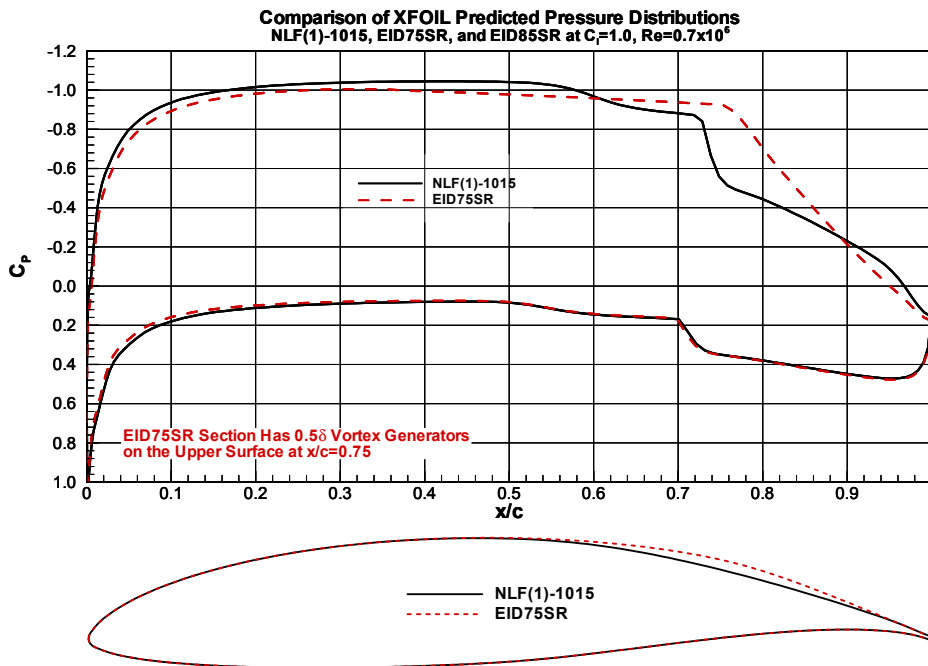
Figure 8: Comparisons of XFOIL predicted pressure distributions for the extended laminar run section EID75SR and the NLF(1)-1015 sections at $C_l=1.0$ and $Re=0.7x10^6$.

American Institute of Aeronautics and Astronautics

Comparison of XFOIL Predicted NLF(1)-1015 and EID75SR Results
Re=0.70x10^6
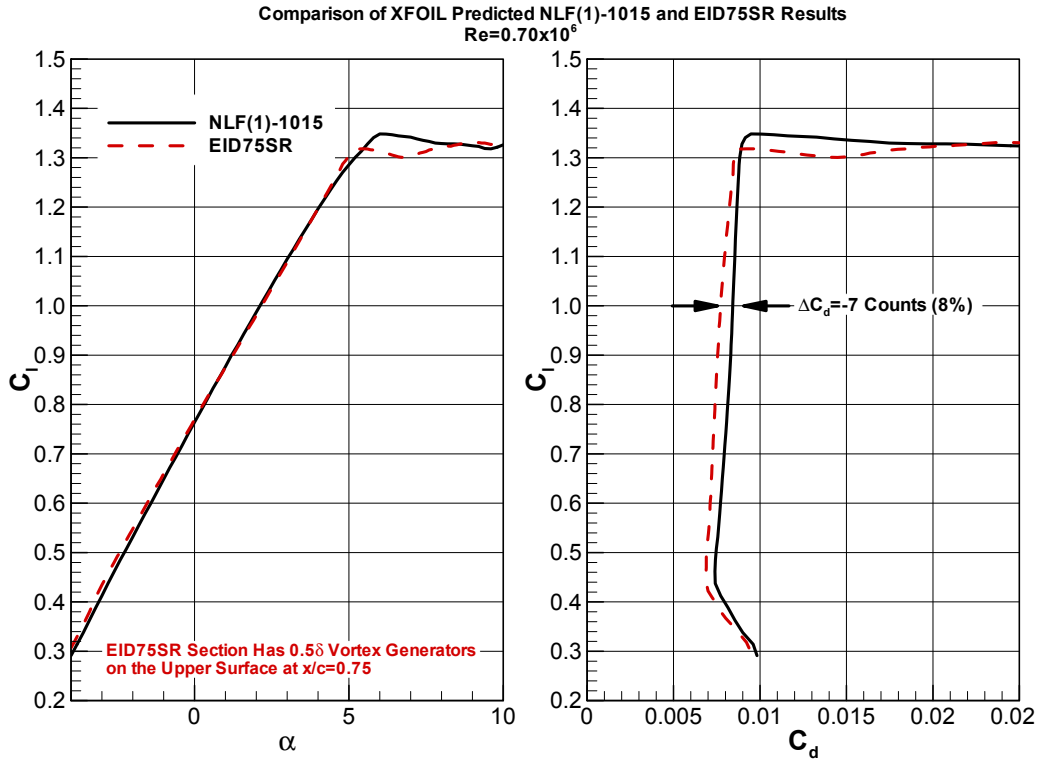
Figure 9: Comparison of predicted XFOIL results on the baseline NLF(1)-1015 and extended laminar EID75SR sections at Re=0.7x10^6.

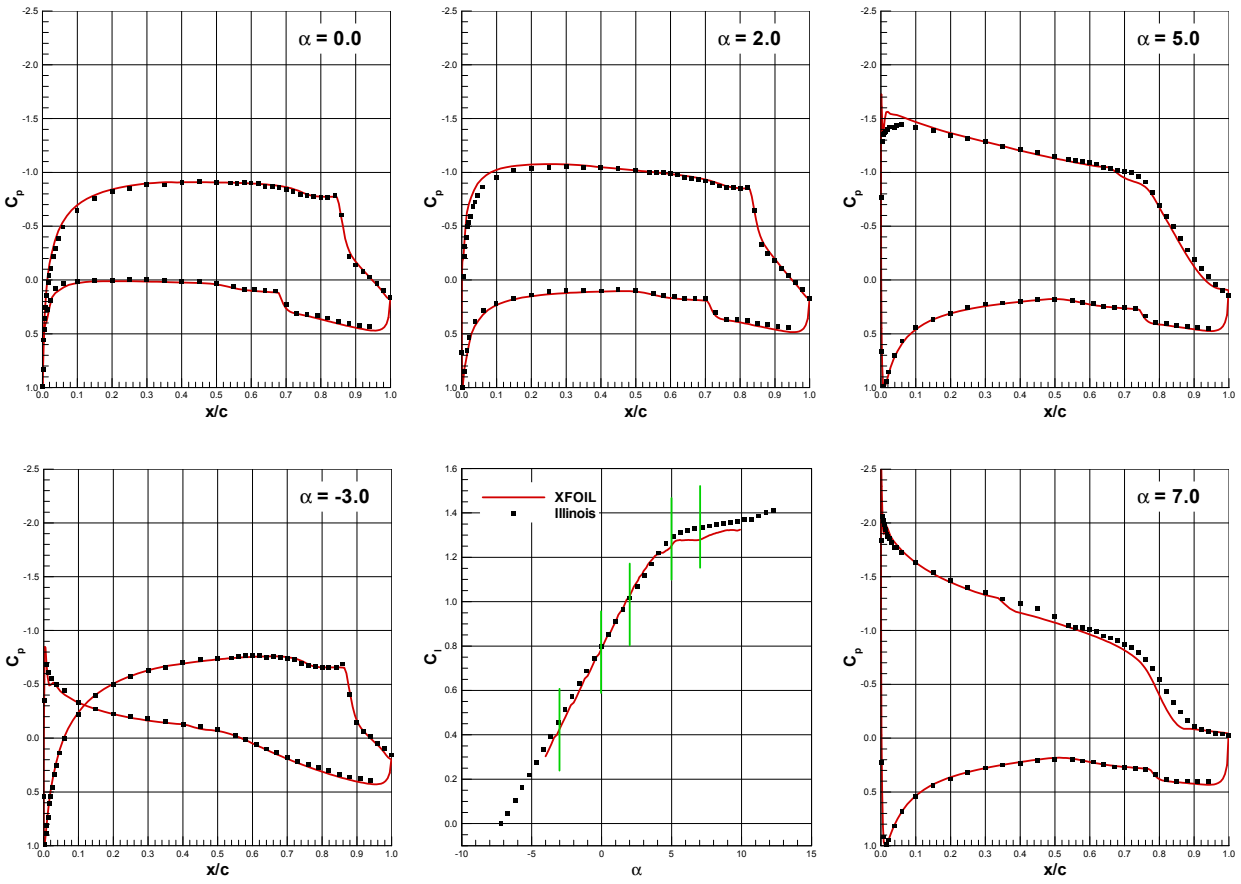**Comparison of XFOIL Predicted and Experimental Clean EID75SR Section Results**
M=0.07, Re=0.7x10^6
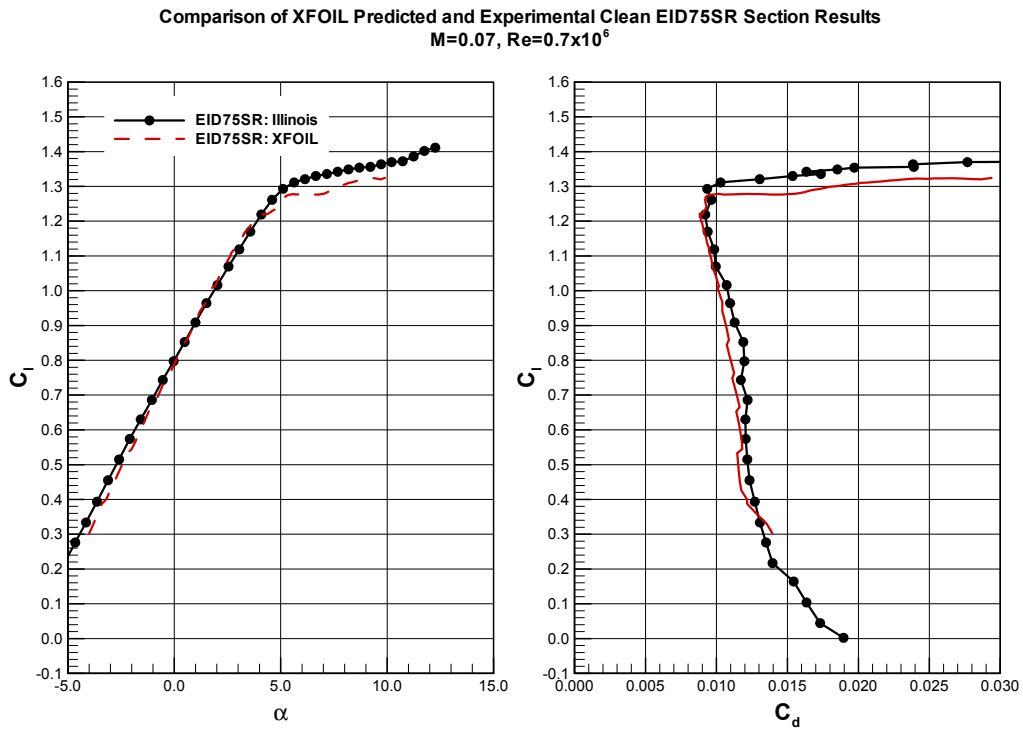
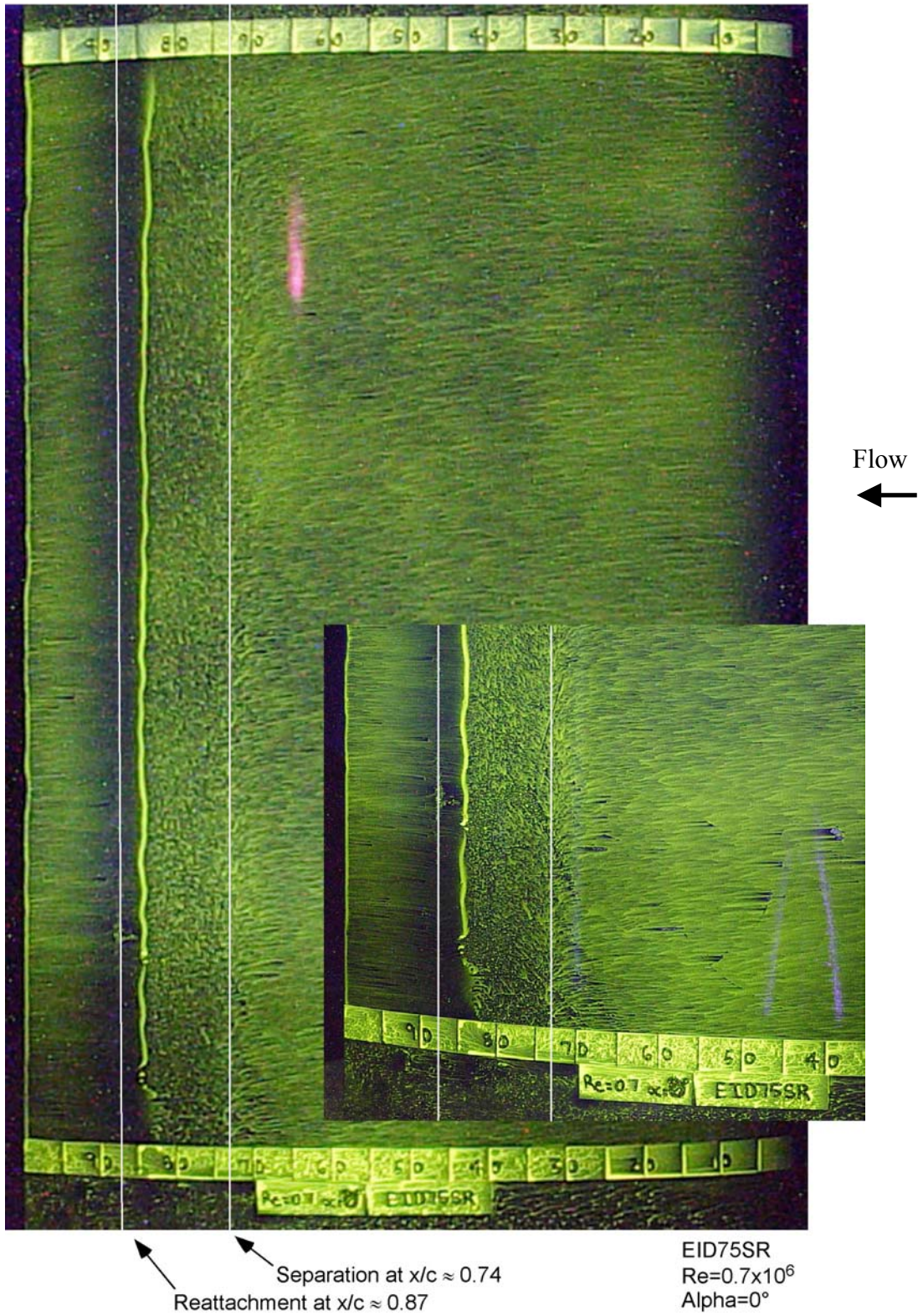*Figure 10: Comparison of XFOIL predicted and experimental results for the clean EID75SR section at Re=0.7x10^6.*

13

Figure 11: Comparison of XFOIL predicted and experimental pressures for the clean EID75SR section at Re=0.7x10⁶.

Figure 12: Fluorescent oil flow visualization of the clean EID75SR section at a=0, Re=0.7x106 showing laminar separation and reattachment.
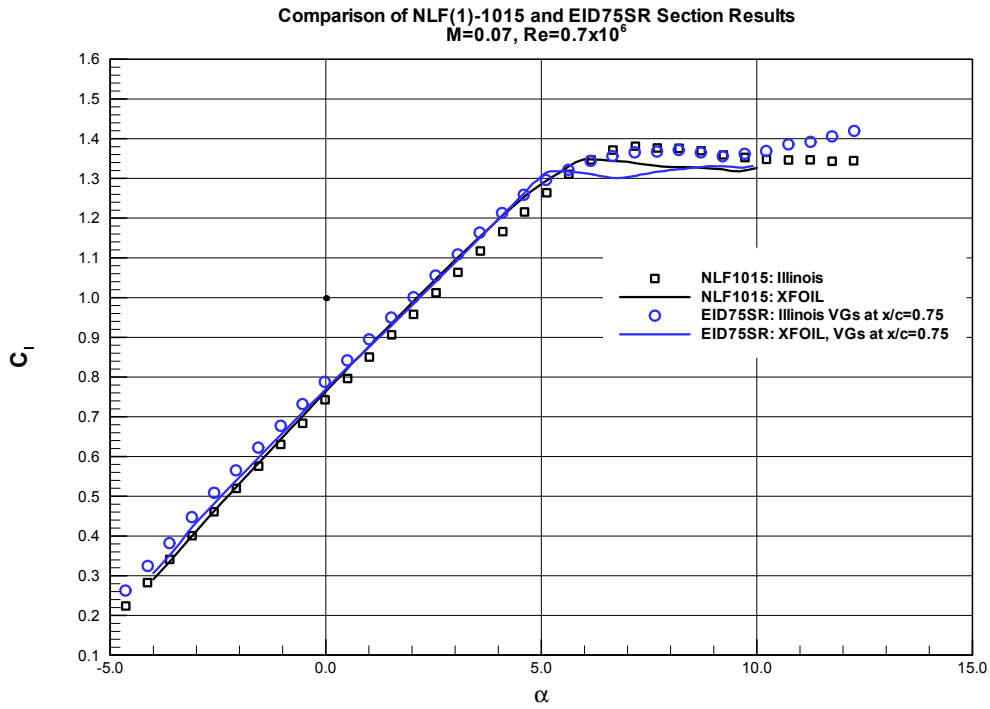
Flow

Separation at x/c ≈ 0.74
Reattachment at x/c ≈ 0.87

EID75SR
Re=0.7x10^6
Alpha=0°

American Institute of Aeronautics and Astronautics

Figure 13: Comparison of modified XFOIL and experimental lift curve results for the baseline NLF(1)-1015 and EID75SR section with co-rotating 0.5δ VGs at x/x=0.75, Re=0.7x10⁶.

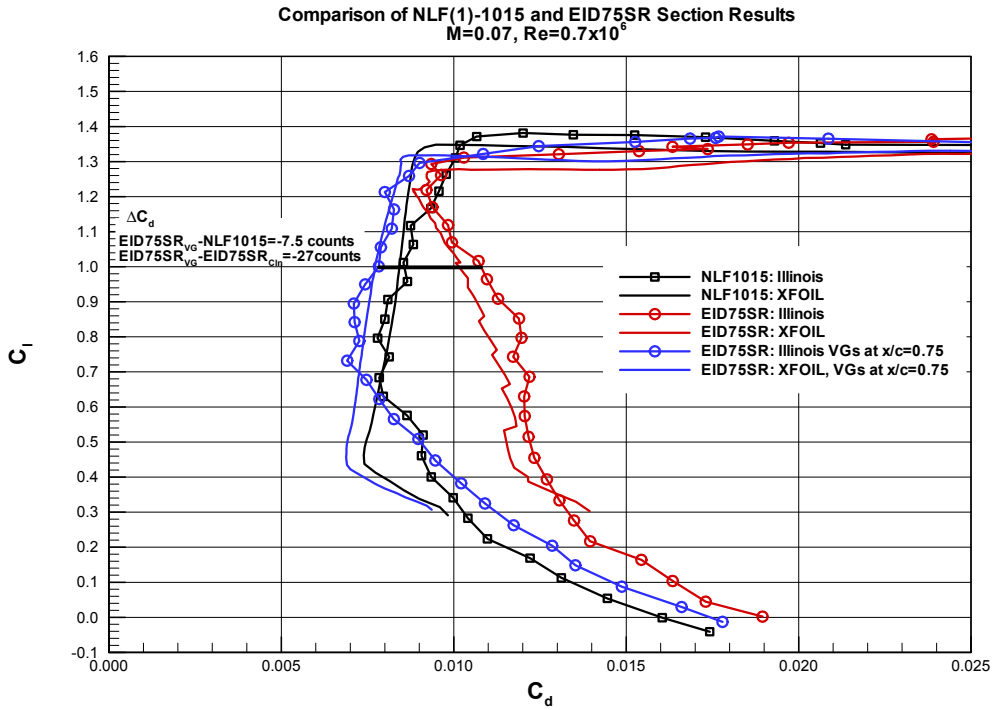*Figure 14: Comparison of modified XFOIL and experimental lift curve results for the baseline NLF(1)-1015 and EID75SR section with co-rotating 0.5δ VGs at x/x=0.75, Re=0.7x10⁶.*
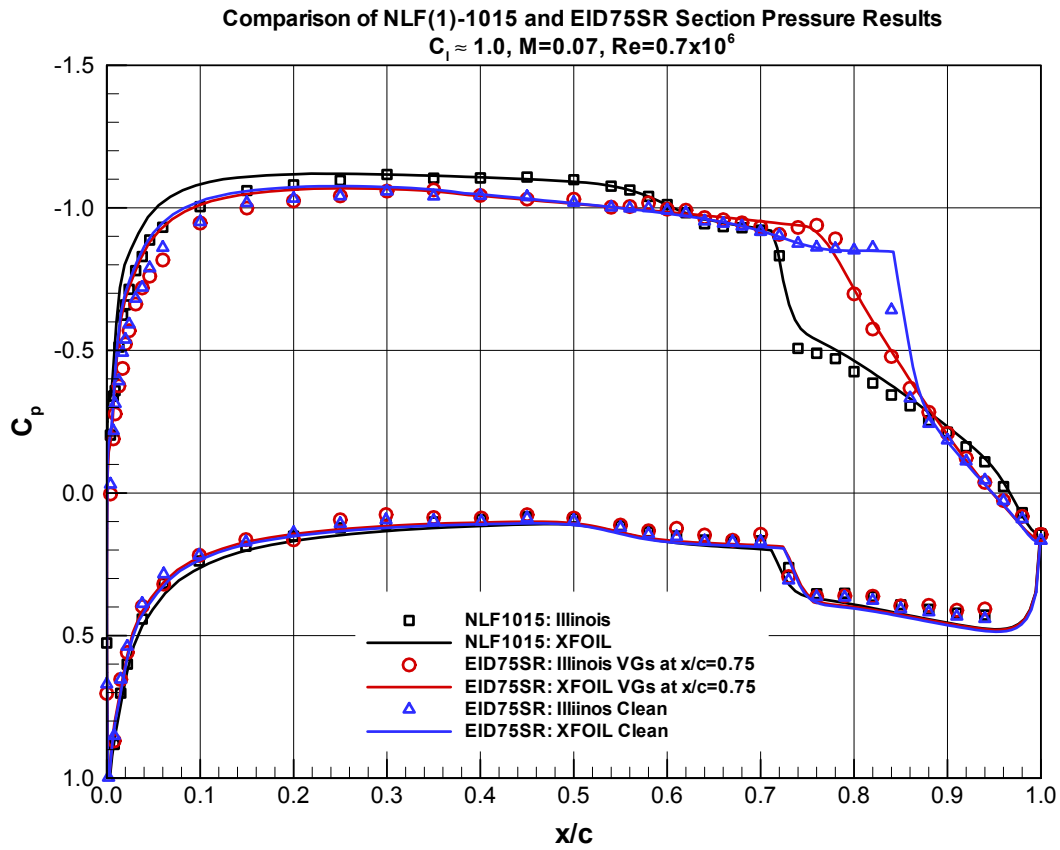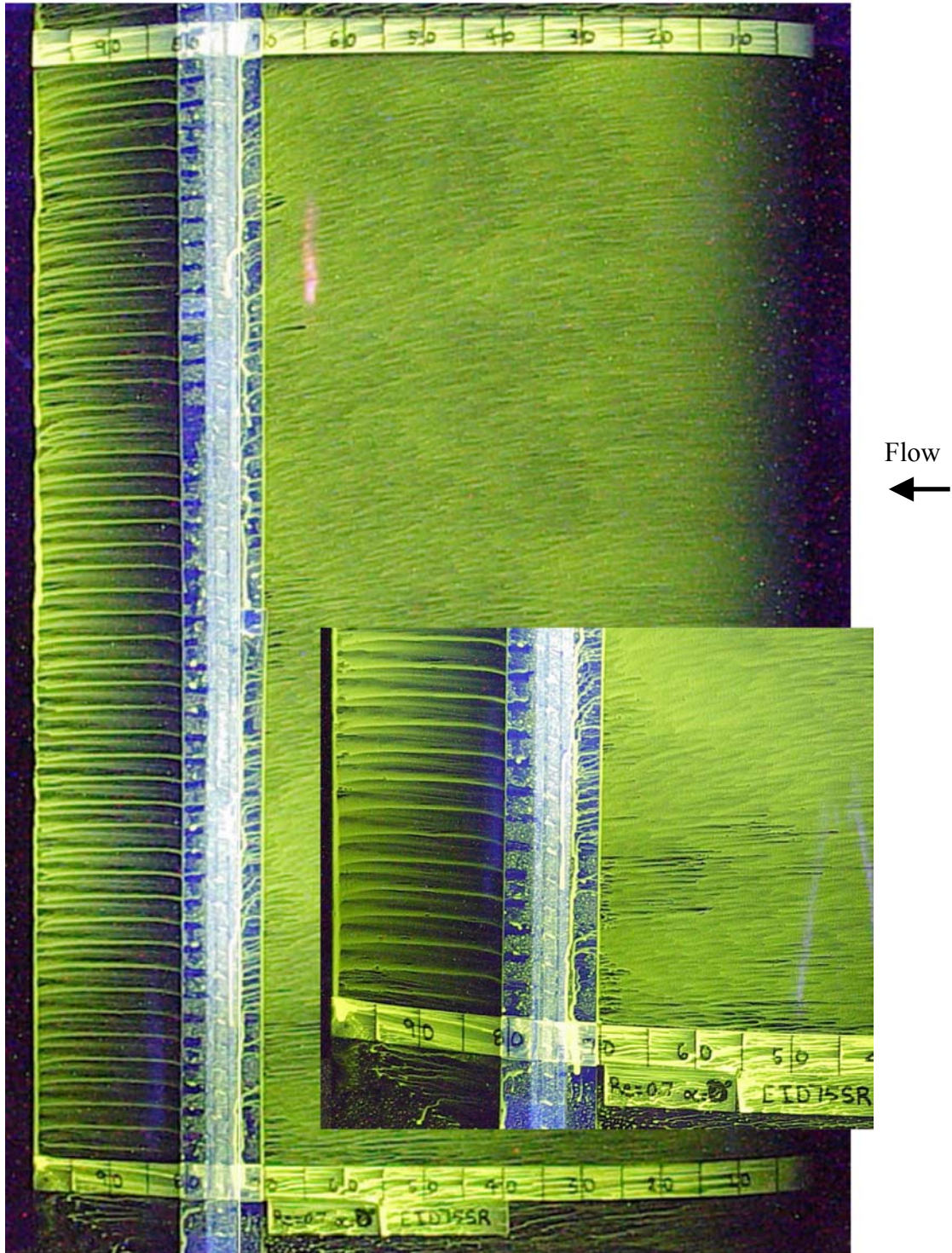
16

American Institute of Aeronautics and Astronautics

Figure 15: Comparison of XFOIL and experimental surface for the NLF(1)-1015 section and the EID75SR section with and without VGs at C_l=1.0, Re=0.7x10^6

Flow

EID75SR
Re=0.7x10^6
Alpha=0°
0.5δ Co- Rotating
VGs at x/c=0.75

Figure 16: Fluorescent oil flow visualization of the EID75SR section at $\alpha=0°$, Re=0.7x10^6 with 0.5δ co-rotating VGs at x/c=0.75.

American Institute of Aeronautics and Astronautics